Nuclear structure insights into reactor antineutrino spectra

A. A. Sonzogni, T. D. Johnson, and E. A. McCutchan

Phys. Rev. C **91**, 011301 — Published 8 January 2015

DOI: 10.1103/PhysRevC.91.011301

Nuclear Structure Insights on Reactor Antineutrino Spectra

A.A. Sonzogni,[1] T.D. Johnson,[1] and E.A. McCutchan[1]

[1] *National Nuclear Data Center, Brookhaven National Laboratory, Upton, NY 11973-5000, USA*

Antineutrino spectra following the neutron induced fission of ^{235}U, ^{238}U, ^{239}Pu, and ^{241}Pu are calculated using the summation approach. While each system involves the decay of more than 800 fission products, the energy region of the spectra most relevant to neutrino oscillations and the reactor antineutrino anomaly is dominated by less than 20 nuclei, for which we provide a priority list to drive new measurements. The very high energy portion of the spectrum is mainly due to the decay of just two nuclides, ^{92}Rb and ^{96}Y. The integral of the signal measured by antineutrino experiments is found to have a dependence on the mass and proton number of the fissioning system. In addition, we observe that $\sim$ 70% of the signal originates from the light fission fragment group and about 50% from the decay of odd-Z odd-N nuclides.

The first measurements of θ_{13} from the Daya Bay [1], RENO [2], and Double Chooz [3] experiments, the proposition of a "reactor antineutrino anomaly" [4], and the use of antineutrino monitoring for nuclear safeguards [5] have underscored the need to precisely understand the complete antineutrino spectra from fissioning systems and have revitalized the field of antineutrino calculations pioneered by P. Vogel *et al.* [6] over 30 years ago. Much effort has focused on the reactor antineutrino anomaly which arose from improved calculations [7] of the antineutrino spectra derived from a combination of information from nuclear databases with reference β spectra [8–10] measured at the Institut Laue-Langevin (ILL) in Grenoble, France. This new approach resulted in an upward shift of about +3% in the overall normalization, an effect which was subsequently confirmed in an independent analysis [11] of the antineutrino flux. Recently, a new analysis [12] including a more complete set of absolute reactor antineutrino flux measurements verified a deficit in detected antineutrinos. A new investigation [13] into the uncertainties associated with the flux prediction, has determined that omitting the corrections to the spectra due to forbidden decays can introduce up to 4% uncertainty in the predicted shape of the antineutrino flux.

There are two general approaches used to calculate antineutrino spectra. The so-called conversion method relies on the measured β spectra from the ILL [8–10], which are fit with a set of virtual β branches and then converted into the corresponding antineutrino spectra. The summation (or ab-initio) method makes use of all available information on the β decays of each fission fragment, summing each nuclide's individual β spectrum weighted by its yield in fission. The former provides the most precise result, as the uncertainties are driven by the uncertainties on the ILL reference spectrum. The latter, at present, has significantly larger uncertainties due to uncertainties in both the decay data and the fission yields. Furthermore, there are known deficiencies in the available decay data [14] and high quality measurements [15] have been shown to have a significant impact on the summation predictions.

While the summation method cannot currently produce high-precision predictions of the antineutrino spectra, there is still much value in the approach as it is intimately connected to the underlying nuclear structure physics. The purpose of the present work is to use the summation method to identify which nuclei are the main contributors to the spectrum and assess the quality of their decay data. This will serve to provide guidance to the experimental nuclear structure community as to which nuclei can be targeted to address deficiencies in decay decay. A similar high-priority list [16] of nuclei relevant to decay heat has already proved useful in improving [17] such calculations and motived large campaigns of experimental study [18]. In addition, we analyze the integral of the signal measured by antineutrino experiments, identifying systematic trends and again, linking the behavior to the underling nuclear structure physics.

In the summation method [6], for a system in equilibrium, the total antineutrino spectra is given by

$$I(E_{\overline{\nu}}) = \sum CFY_i \times I_i(E_{\overline{\nu}}), \tag{1}$$

where CFY_i is the cumulative fission yield and $I_i(E_{\overline{\nu}})$ is the antineutrino spectrum from the i^{th} beta-decaying nucleus (either from its ground or possibly isomeric state) in the network, which is calculated as

$$I_i(E_{\overline{\nu}}) = \sum br_{ik} \times I_{ik}(E_{\overline{\nu}}), \tag{2}$$

where br_{ik} is the branching ratio to the daughter level with energy E_k and $I_{ik}(E_{\overline{\nu}})$ is the antineutrino spectra for a single transition with end point energy $Q_\beta - E_k$. In the present work, the cumulative fission yields are taken from the JEFF-3.1 library [19] and the decay data are taken from an updated version of the ENDF/B-VII.1 library [20]. The major change to the decay data library is that, when available, we have used branching ratio data from TAGS experiments [21, 22]. In addition, we use the direct β-spectrum measurements of Rudstam *et al.* [23] to obtain $I_i(E_{\overline{\nu}})$ for ten nuclides without TAGS data and with incomplete decay schemes. Finally, the ENDF/B-VII.1 decay data sub-library includes theoretical calculations [24] of β- spectra for the most neutron rich nuclides with incomplete decay schemes. Due to limitations in the library's format, the antineutrino spectra are not part of

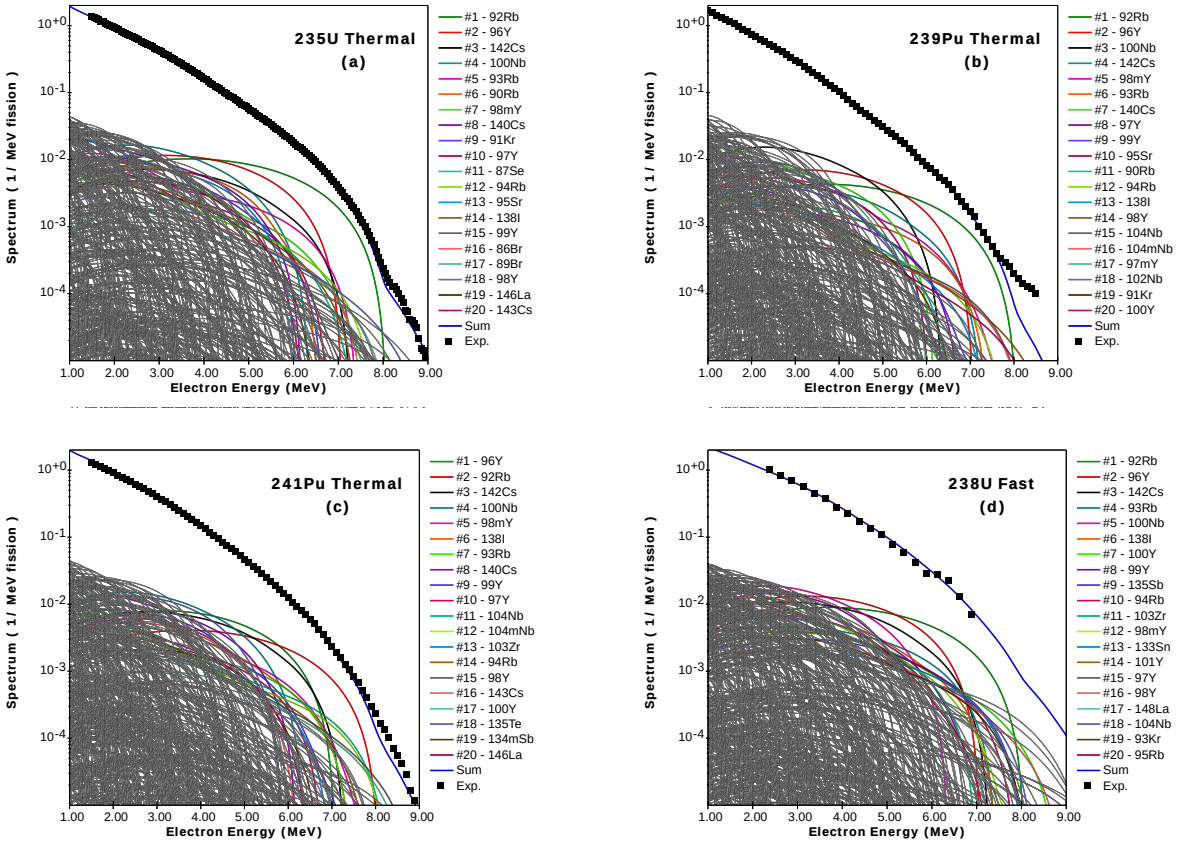

FIG. 1. (Color online) Calculated electron spectra (solid blue line) following the thermal fission of (a) ^{235}U, (b) ^{239}Pu, (c) ^{241}Pu, and (d) the fast fission of ^{238}U, compared with the high-resolution data from ILL [25] as well as the recently published data for ^{238}U [26] (black squares). The thin grey lines indicate the individual beta spectrum from each fission fragment, $I_i(E_{\overline{\nu}})$, and thick colored lines highlight the 20 most important individual contributors at 5.5 MeV.

TABLE I. β-decay Q value, ground state to ground state branching ratio and cumulative fission yields for ^{92}Rb and ^{96}Y.

Nuclide	Q_β (MeV)	Branching Ratio (%)	^{235}U CFY (thermal)	^{238}U CFY (fast)	^{239}Pu CFY (thermal)	^{241}Pu CFY (thermal)
^{92}Rb	8.095	95.2 ± 0.7	0.048	0.042	0.020	0.019
^{96}Y	7.103	95.5 ± 0.5	0.047	0.053	0.029	0.032

the official ENDF/B-VII.1 release, but were nevertheless included in our calculations.

The beauty of the summation method, is that the individual effect of each of the 800 or so different fission fragments on the overall antineutrino spectrum can be investigated. We exploit this in Fig. 1, decomposing the total beta-minus spectrum into the individual beta-spectra for each fission fragment. The thin gray lines indicate the individual beta spectrum from each fission fragment, $I_i(E_{\overline{\nu}})$, while the thick colored lines highlight the 20 most important individual contributors at 5.5 MeV. Also included in Fig. 1 are the experimentally measured total beta-spectra (black squares) [25, 26] compared with the summed spectra from the present work (solid blue line). What is remarkable is that given the complexity of the overall calculation and the vast number of nuclides contributing, at the higher energies only a handful of nuclei significantly influence the spectrum. Particularly in the case of ^{235}U and ^{238}U, two nuclei stand out predominately at high energies, ^{92}Rb and ^{96}Y. This is due to a combination of a large cumulative fission yield, a large beta minus Q-value and a large ground state to ground state β-feeding intensity. These properties are listed in Table I. For ^{239}Pu and ^{241}Pu, the contributions from ^{92}Rb and ^{96}Y are reduced somewhat due to their smaller cumulative fission yield.

Given the significance of ^{92}Rb and ^{96}Y to the antineutrino spectrum calculations, we investigate further the quality and reliability of their decay data. Both mainly undergo first forbidden, $0^- \rightarrow 0^+$ ground state to ground

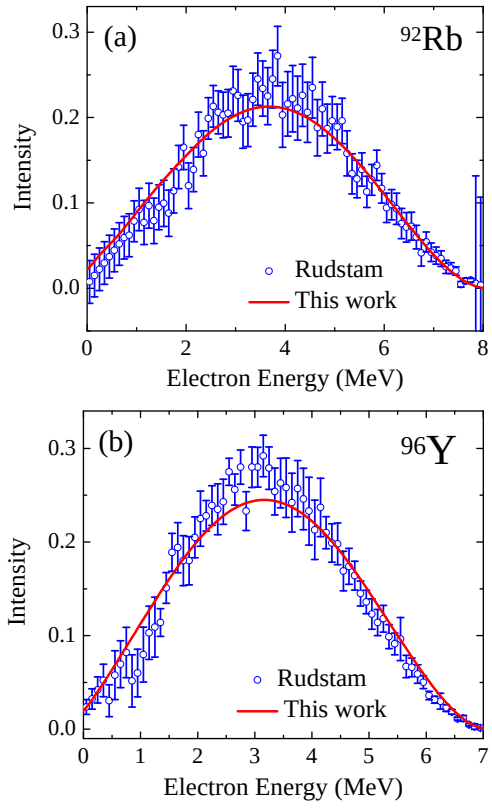

FIG. 2. (Color online) Comparison of the measured β spectrum [23] with present calculations for (a) ^{92}Rb and (b) ^{96}Yb using a 95% ground state β-feeding intensity and assuming an allowed shape.

state transitions. While the ground state β-feeding intensity for ^{96}Y is considered to be reliable [27], there have been conflicting reports for that of ^{92}Rb. For many years, the accepted value [28] was ∼50%, only recently updated [29] to 95% based on the work by G. Lhersonneau *et al.,* [30]. We note that the ENDF/B-VII.1 library has a ∼50% branch which we have updated for the present calculations. As mentioned previously, Rudstam *et al.,* [23] directly measured the β spectrum for a number of fission products. In Fig. 2, we compare those measurements for ^{92}Rb and ^{96}Y with our calculations for the β spectrum using the ground state to ground state β-feeding intensities given in Table I and assuming an allowed shape for all transitions. The agreement is quite good, supporting the ∼95% ground state to ground state branch in both nuclei. Fig. 2 further highlights that our current knowledge of β-spectra from fission products is fairly poor. Most precision spectra have only been measured for nuclides close to the valley of stability, and hence with considerably lower Q-values. The allowed shape used in our calculations agrees well with the data given the present level of uncertainties. Far more precise experiments are needed to test the predictions of Ref. [13] and determine whether these first-forbidden transitions should be calculated with additional shape factors.

TABLE II. Strongest contributors to the antineutrino spectrum from ^{235}U in the energy range around 4.0 MeV. Included are the β decay Q value, the ground state to ground state β-feeding intensity (GS BR), the initial and final J^π of the ground states (all from Ref. [32]), and the percent contribution to the antineutrino spectra (Contr.).

Nuclide	Q_β (MeV)	GS BR (%)	$J^\pi_{gs} \rightarrow J^\pi_{gs}$	Contr. %
^{96}Y	7.1	95.5(5)	$0^- \rightarrow 0^+$	6.3
^{92}Rb	8.1	95.2(7)	$0^- \rightarrow 0^+$	6.1
^{100}Nb	6.4	50(7)	$1^+ \rightarrow 0^+$	5.5
^{135}Te	5.9	62(3)	$(7/2^-) \rightarrow 7/2^+$	3.7
^{142}Cs	7.3	56(5)	$0^- \rightarrow 0^+$	3.5
^{140}Cs	6.2	36(2)	$1^- \rightarrow 0^+$	3.4
^{90}Rb	6.6	33(4)	$0^- \rightarrow 0^+$	3.4
^{95}Sr	6.1	56(3)	$1/2^+ \rightarrow 1/2^-$	3.0
^{88}Rb	5.3	77(1)	$2^- \rightarrow 0^+$	2.9

TABLE III. Same as Table II, except the strongest contributors from ^{235}U at 5.5 MeV are summarized.

Nuclide	Q_β (MeV)	GS BR (%)	$J^\pi_{gs} \rightarrow J^\pi_{gs}$	Contr. %
^{92}Rb	8.1	95.2(7)	$0^- \rightarrow 0^+$	21.6
^{96}Y	7.1	95.5(5)	$0^- \rightarrow 0^+$	14.5
^{142}Cs	7.3	56(5)	$0^- \rightarrow 0^+$	6.8
^{100}Nb	6.4	50(7)	$1^+ \rightarrow 0^+$	4.7
^{93}Rb	7.5	35(3)	$5/2^- \rightarrow 7/2^+$	4.6
^{90}Rb	6.6	33(4)	$0^- \rightarrow 0^+$	3.4
^{98m}Y	9.0	12(5)[a]	$(4,5) \rightarrow 4^+$	2.8
^{140}Cs	6.2	36(2)	$1^- \rightarrow 0^+$	2.4
^{91}Kr	6.8	18(3)[b]	$5/2^{(+)} \rightarrow (5/2^-)$	2.4

[a] Strongest branch to a low-lying state is to a 4^+, 1843-keV level.
[b] Strongest branch is to a $(5/2^-)$, 109-keV level.

The ^{92}Rb cumulative fission yield following the thermal fission of ^{235}U definitely merits a new measurement. While both the ENDF/B and JEFF values of 0.048 agree within 0.3%, it has been reported to be 0.074 (11) by Tipnis *et al.*, [31], that is, 50% larger than the JEFF value, which would mean that at 5.5 MeV, ^{92}Rb would contribute about 30% of the total electron spectra.

There are several additional nuclei which strongly influence the antineutrino spectrum, as evidenced by the colored lines in Fig. 1 which are an order of magnitude larger than the sea of thin grey lines. In Tables II and III we provide the list of top contributors to the spec-

tra at 4.0 MeV and 5.5 MeV for ^{235}U. Similar tables for ^{239}Pu, ^{241}Pu and ^{238}U are given in the supplemental information accompanying this article [33]. Again, those nuclei which strongly influence the spectrum exhibit a consistent set of properties: large Q_β values, large cumulative fission yields, and large ground state to ground state β-feeding intensities. A precise measurement of the ground-state β feeding intensity is the key experimental quantity. As most of these β-decay transitions are first-forbidden, high-precision β spectrum measurements to determine the significance of a shape correction factor would also be useful. Despite the fact that the complete problem involves data on over 800 nuclei, the nuclei in Tables II and III comprise $\sim$ 40% and 60% of the total spectrum at 4.5 and 5.5 MeV, respectively. This likens the experimental problem to that of the priority list for decay heat [16] and a targeted experimental campaign could yield significant improvements on our ability to calculate antineutrino spectra via the summation method.

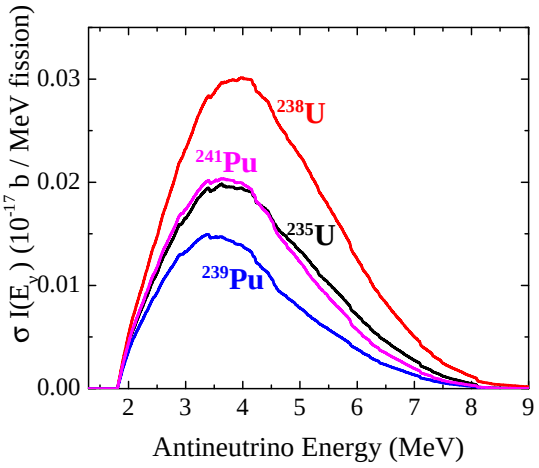

FIG. 3. (Color online) Antineutrino spectra multiplied by the $\overline{\nu} + p \rightarrow n + e^+$ cross section for the thermal fission of ^{235}U, ^{239,241}Pu and the fast fission of ^{238}U.

Neutrino oscillation experiments, like Daya Bay, measure the product of the antineutrino spectrum multiplied by the cross section, σ, for inverse beta decay, $\overline{\nu}$+proton $\rightarrow$ neutron $+e^+$. Using the cross section from Ref. [34], we obtain the results shown in Fig. 3. Important differences are observed for the four different fission sources, both in magnitude and shape. ^{238}U yields the most events and with higher average energy while ^{239}Pu produces fewer events with smaller average energy. The shoulder at about 5 MeV, which we interpret as mainly due to ^{96}Y and ^{92}Rb, is more prominent for ^{235}U and ^{238}U.

For neutrino oscillation studies, the relevant quantity is the integral over energy of the cross section multiplied by the neutrino spectrum, $<\sigma I_{\overline{\nu}}>$. As can be seen in Fig. 3, this quantity is about the same for ^{235}U and ^{241}Pu, while it is about 50% larger for ^{238}U and 35% smaller for ^{239}Pu. This feature is easily understood by consid-

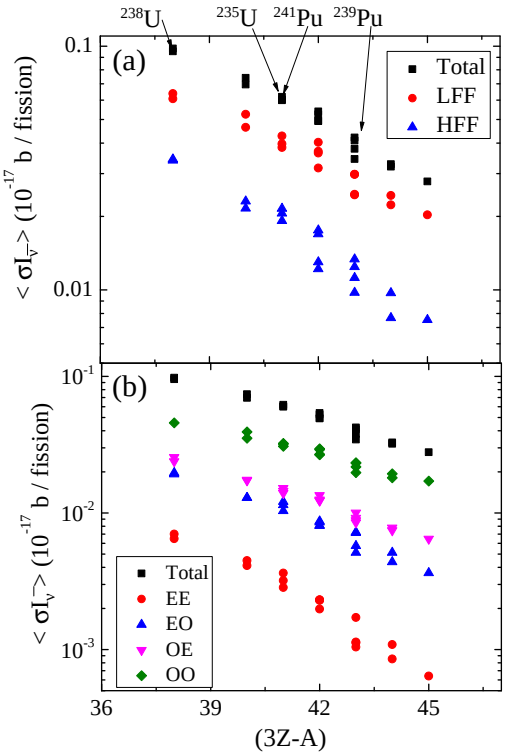

FIG. 4. (Color online) $<\sigma I_{\overline{\nu}}>$ as a function of $(3Z - A)$ for fissioning systems ranging from ^{232}Th to ^{245}Cm. (a) The total, as well as the contribution from the light fission fragments (LFF) and heavy fission fragments (HFF) are shown. (b) Same as (a), except the individual contributions from nuclides with even-even (EE), even-odd (EO), odd-even (OE) and odd-odd (OO) combinations of protons and neutrons are indicated.

ering the distribution of fission products populated by each of the fissioning systems. Comparing, for example ^{235}U and ^{238}U, the main difference is that the ^{238}U fission fragment distribution is shifted to more neutron-rich nuclides. This then results in more antineutrinos being emitted while the fragments decay back to stability, and with larger energies, as beta-decay Q values generally increase with increasing neutron number. As mentioned before, we have used theoretical spectra for nuclides with incomplete decay schemes. We note that these spectra contribute about 4%, 14%, 7% and 12% of $<\sigma I_{\overline{\nu}}>$ for ^{235}U, ^{238}U, ^{239}Pu and ^{241}Pu, respectively.

To study the dependence of $<\sigma I_{\overline{\nu}}>$ in a more quantitative manner, we apply a simple quantity commonly used [35] to parameterize properties of a fissioning system: $(3Z\text{-}A)$ where Z is the proton number and A the number of nucleons of the fissioning nucleus. Traditionally, a $(3Z\text{-}A)$ dependence is used to parameterize [36, 37] the delayed neutron yield from fissioning systems, while here we study its relevance to the antineutrino spectrum. In Fig. 4 we explore the logarithmic dependence of $<\sigma I_{\overline{\nu}}>$ on $(3Z\text{-}A)$ for a variety of systems ranging from ^{232}Th to ^{245}Cm. A clear linear dependence is observed. A similar

linear dependence is obtained for the average antineutrino energy as a function of ($3Z$-A). In Fig. 4(a), the $<\sigma I_{\overline{\nu}}>$ values are separated into the contribution from light ($Z \leq 47$) and heavy fission fragments. The surprising feature is that the light group accounts for nearly 70% of $<\sigma I_{\overline{\nu}}>$ for all the systems. In Fig. 4 (b) the $<\sigma I_{\overline{\nu}}>$ values are separated into the contributions from nuclides with different combinations of even and odd neutron and proton number. As one may expect, odd-Z, odd-N nuclides are the main contributors with about 50% of the total $<\sigma I_{\overline{\nu}}>$. This is because these nuclides have the largest Q_β values and typically have one low-spin, long-lived level feeding directly the ground state of the even-even daughter. On the other hand, due to the relatively low Q_β values, even-Z, even-N nuclides only contribute about 5% to $<\sigma I_{\overline{\nu}}>$.

In summary, we have combined fission yield data from JEFF-3.1 and decay data from ENDF/B-VII.1 to calculate antineutrino spectra for the four most important fuels of commercial nuclear reactors, ^{235}U, ^{238}U, ^{239}Pu, and ^{241}Pu. The antineutrino spectra from these four actinides are noticeably different, both in multiplicity and average energy. By decomposing the spectrum into the contribution from individual nuclides, the shoulder observed on the high energy half of the spectra is found to be mainly due to the decay of two nuclides, ^{92}Rb and ^{96}Y. Furthermore, while the total problem involves the contribution of more than 800 nuclides, the antineutrino spectrum in the relevant energy region is dominated by less than 20 nuclei, of which we provide a priority list to hopefully stimulate new measurements. We find about 65-70% of the cross section averaged antineutrino spectrum originates from the light fission fragments. The decay from odd-Z, odd-N nuclides represents about 50% of this quantity, while even-Z, even-N nuclides only contribute about 4-7%. Finally, similar to delayed neutron multiplicity, we find that the logarithm of the cross section averaged antineutrino spectra exhibits a linear dependence with $(3Z - A)$ for a number of fissioning systems.

We have chosen the JEFF-3.1 fission yields and an updated ENDF/B-VII.1 decay data sub-library for the present calculations as they provide the most up-to-date evaluation of currently available data. While other libraries might produce differences in the fine details of the calculations, the above points highlight the underlying physics and thus, should remain true under other combinations of current libraries.

We are grateful to Prof. K. Schreckenbach for providing us the high resolution ILL data and to the Institute for Nuclear Theory at the University of Washington for hosting a Workshop on Reactor Antineutrinos [38] where some of these results were presented. This work was sponsored by the Office of Nuclear Physics, Office of Science of the U.S. Department of Energy under Contract No. DE-AC02-98CH10886.

[1] F.P. An *et al.*, Phys. Rev. Lett. **108**, 171803 (2012).
[2] J.K. Ahn *et al.*, Phys. Rev. Lett. **108**, 191802 (2012).
[3] Y. Abe *et al.*, Phys. Rev. Lett. **108**, 131801 (2012).
[4] G. Mention *et al.,* Phys. Rev. D **83**, 073006 (2011).
[5] E. Christensen, P. Huber, P. Jaffke, and T.E. Shea, Phys. Rev. Lett. **113**, 042503 (2014).
[6] P. Vogel, G.K. Schenter, F.M. Mann, and R.E. Schenter, Phys. Rev. C **24**, 1543 (1981).
[7] Th. A. Mueller *et al.,* Phys. Rev. C **83**, 054615 (2011).
[8] F. von Feilitzsch, A.A. Hahn, and K. Schreckenbach, Phys. Lett. B **118**, 162 (1982).
[9] K. Schreckenbach, G. Colvin, W. Gelletly, and F. von Feilitzsch, Phys. Lett. B **160**, 325 (1985).
[10] A.A. Hahn *et al.,* Phys. Lett. B **218**, 365 (1989).
[11] P. Huber, Phys. Rev. C, **84** 024617 (2011).
[12] C. Zhang, Z. Qian, and P. Vogel, Phys. Rev. D **87**, 073018 (2013).
[13] A.C. Hayes *et al.,* Phys. Rev. Lett **112**, 202501 (2014).
[14] J.C. Hardy *et al.,* Phys. Lett. B **71**, 307 (1977).
[15] M. Fallot *et al.*, Phys. Rev. Lett. **109**, 202504 (2012).
[16] IAEA 499, INDC(NDS)-0499, NEA Data Bank, Paris, May 3, 2006.
[17] A. Algora *et al.,* Phys. Rev. Lett. **105**, 202501 (2010).
[18] K.P. Rykaczewski, Nucl. Data Sheets **120**, 16 (2014).
[19] M.A. Kellett, O. Bersillon, and R.W. Mills, JEFF REPORT 20, OECD, ISBN 978-92-64-99087-6 (2009).
[20] M.B. Chadwick *et al.*, Nucl. Data Sheets **112**, 2887 (2011).
[21] R.C. Greenwood *et al.*, Nucl. Instrum. Methods Phys. Res. A **390**, 95 (1997).
[22] D. Jordan *et al.*, Phys. Rev. C **87**, 044318 (2013).
[23] G. Rudstam *et al.*, At. Data Nucl. Data Tables **45**, 239 (1990).
[24] T. Kawano, P. Moller, and W.B. Wilson, Phys. Rev. C **78**, 054601 (2008).
[25] K. Schreckenbach, private communication (2012).
[26] N. Haag *et al.,* Phys. Rev. Lett. **112**, 122501 (2014).
[27] D. Abriola and A.A. Sonzogni, Nucl. Data Sheets **109**, 2501 (2008).
[28] C.M. Baglin, Nucl. Data Sheets **91**, 423 (2000).
[29] C.M. Baglin, Nucl. Data Sheets **113**, 2187 (2012).
[30] G. Lhersonneau *et al.*, Phys.Rev. C **74**, 017308 (2006).
[31] S.V. Tipnis *et al.,* Phys. Rev. C **58**, 905 (1998).
[32] http://www.nndc.bnl.gov/ensdf
[33] See Supplemental Material at [URL will be inserted by publisher] for tables of the top twenty contributors to the antineutrino spectra for ^{235}U, ^{238}U, ^{239}Pu, and ^{241}Pu at antineutrino energies around 4.0 MeV and 5.5 MeV.
[34] A. Strumia and F. Vissani, Phys. Lett. B **564**, 42 (2003).
[35] G. Moscati and J. Goldemberg, Phys. Rev. **126**, 1098 (1962).
[36] H.L. Pai, Ann. Nucl. Energy **3**, 125 (1976).
[37] D.J. Loaiza, G. Brunson, R. Sanchez, and K. Butterfield, Nucl. Sci. Eng. **128**, 270 (1998).
[38] http://www.int.washington.edu/PROGRAMS/13-3/workshop.html